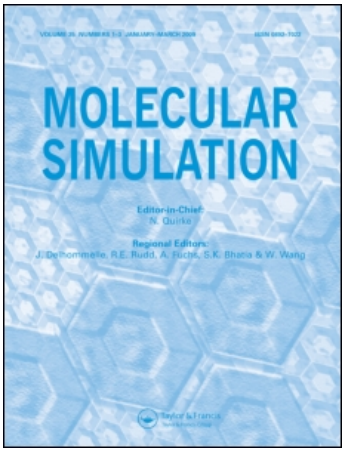

Molecular Simulation
Publication details, including instructions for authors and subscription information:
http://www.informaworld.com/smpp/title~content=t713644482

Simulations of glasses: multiscale modeling and density of states Monte-Carlo simulations

J. Ghosh[a]; B. Y. Wong[a]; Q. Sun[a]; F. R. Pon[b]; R. Faller[a]
[a] Department of Chemical Engineering & Materials Science, UC Davis, Davis, CA, USA [b] Intel, Folsom, CA, USA

To cite this Article Ghosh, J. , Wong, B. Y. , Sun, Q. , Pon, F. R. and Faller, R.(2006) 'Simulations of glasses: multiscale modeling and density of states Monte-Carlo simulations', Molecular Simulation, 32: 3, 175 — 184
To link to this Article: DOI: 10.1080/08927020600592985
URL: http://dx.doi.org/10.1080/08927020600592985

Molecular Simulation, Vol. 32, Nos. 3–4, 15 March–April 2006, 175–184

Taylor & Francis
Taylor & Francis Group

Simulations of glasses: multiscale modeling and density of states Monte-Carlo simulations

J. GHOSH†, B. Y. WONG†, Q. SUN†, F. R. PON†‡ and R. FALLER†*

†Department of Chemical Engineering & Materials Science, UC Davis, Davis, CA 95616, USA
‡Intel, Folsom, CA 95630, USA

(Received November 2005; in final form January 2006)

We show the application of two recent developments in molecular simulations, density of states (DOS) (Wang–Landau) Monte-Carlo and multiscale modeling, to the understanding of the glass transition.

First, we review DOS Monte-Carlo using the two-dimensional Ising model without external field on lattices of varying size. We point out that we can analyze the resulting densities of state in a canonical and a microcanonical way starting from the same simulations. The heat capacity is discussed in both ensembles. Results from both ensembles of off-lattice simulations of a model binary glass former are compared as well.

Subsequently, a self-consistent systematic mapping procedure for molecular models from the atomistic to the mesoscale is presented. It allows to efficiently derive mesoscale models with fewer interaction centers from atomistic models preserving the molecular identity. We use the optimization of a corresponding mesoscale model for atactic polystyrene (a good glass former) in the melt as an example. Simulations of different temperatures using this model allow some insight into the glass formation of this system.

We point out the strengths and weaknesses of these approaches and give an outlook towards their combination.

Keywords: Monte-Carlo; Molecular dynamics; Density of states; Multiscale modeling; Glasses

1. Motivation

The transition from a liquid to an amorphous solid that occurs upon cooling in some systems and under some circumstances remains one of the largely unresolved problems of statistical physics [1,2]. At the experimental level, this glass transition is generally associated with a strong increase in all relevant relaxation times of the system. This results in a departure of laboratory measurements from equilibrium. A number of theoretical models have been proposed to explain this transition: It may be triggered by an underlying ideal thermodynamic glass transition [3] which is believed to occur at the Kauzmann temperature T_K, where only one minimum energy basin of attraction is accessible to the system. Such a transition has, however, not yet been seen in experiments. This type of argument goes back to Gibbs and diMarzio [4]. Recent studies using replica methods have supported such a transition in Lennard–Jones glass formers [3,5,6]. Experiments and other simulations do not support this view. Notably, simulations of hard disks have failed to detect any evidence of a thermodynamic transition up to extremely high packing fractions [7]. It is not clear if discrepancies in the reported behaviors of different systems are due to fundamental differences. If this is the case, we have to find out which are the decisive characteristics governing the different scenarios. Other theories have attempted to establish a connection between the glass transition and the rapid increase in relaxation times in the vicinity of a theoretical "mode-coupling" temperature T_{MCT} giving rise to a "kinetic" transition [8]. Both viewpoints have received support from molecular simulations [9–12]. Very low temperature simulations have generally been avoided, and extrapolations are routinely used to infer low temperature behavior [5,13–15]. This stems from the fact that simulations near or even below a glass transition are notoriously difficult, and the results must be considered with caution. The relevant time scales below T_{MCT} or T_g (glass transition temperature) are too long to be sampled by conventional molecular dynamics. For Monte-Carlo techniques, it has been difficult to establish what extent available studies have

*Corresponding author. Email: rfaller@ucdavis.edu

Molecular Simulation
ISSN 0892-7022 print/ISSN 1029-0435 online © 2006 Taylor & Francis
http://www.tandf.co.uk/journals
DOI: 10.1080/08927020600592985

succeeded in sampling all relevant regions of phase space, particularly at low temperatures and elevated densities. In order to address fundamental questions of glasses, we require advanced molecular simulation techniques. Two such techniques are presented in this contribution.

2. Introduction

2.1 Density of states Monte-Carlo—statistical mechanical background

Density of states (DOS) Monte-Carlo, or after its inventors Wang–Landau sampling, has been very successful keeping in mind that it is only a few years old [12, 16–23] basing on an earlier idea from de Oliveira *et al.* [24]. For a number of systems, it has been shown that it often is more efficient than traditional Monte-Carlo [12,16,17]. The beauty of the technique is mainly its simplicity, both from a conceptual and an algorithmic standpoint. This makes it appealing to applications in all fields of molecular simulation.

Let us shortly review the fundamentals of Monte-Carlo simulations in general and DOS Monte-Carlo in particular. A Monte-Carlo simulation is based on visiting representative microstates of the system in order to calculate integrals over phase space, for instance, thermodynamic averages or partition functions. At any given point, during the simulation, the system is in one defined microstate p, a single point in phase space and the algorithm then proposes a jump to a new microstate p'. This transition is accepted with a transition probability $\Pi(p, p')$. Otherwise, the original state is counted again. These transition probabilities are normally prescribed in terms of macrostates $P(E)$, which for simplicity in the following discussion depend only on energy. Generalizations to other extensive macroscopic variables (like N or V) are straight forward. Every macrostate corresponds to a phase space volume rather than a single point.

In order for a Monte-Carlo algorithm to be correct, the following rate equation has to be fulfilled at equilibrium

$$\sum_{p'} \pi(p)\Pi(p,p') = \sum_{p'} \pi(p')\Pi(p',p), \quad p \neq p'. \tag{1}$$

Here $\pi(p)$ is the probability of the system to be in state p. This states the obvious prerequisite that for a distribution function to be stationary (i.e. at equilibrium) the number of transitions into and out of a given state have to be equal. In most simulations, actually the stricter and more widely known criterion of detailed balance is observed

$$\pi(p)\Pi(p,p') = \pi(p')\Pi(p',p), \quad p \neq p'. \tag{2}$$

The probability of a macrostate $P(E)$ to be visited can be written as

$$\pi(P(E)) = \pi(E) \propto w(E)\Omega(E) \tag{3}$$

where $\Omega(E)$ is the number of states, i.e. different realizations of the energy E in terms of microstates. Since a macrostate only is characterized by its energy, we can write $\pi(P(E)) = \pi(E)$. The number of states reads

$$\Omega(E) = \iint_{\text{Phasespace}} \delta(E'(\{r,p\}) - E) d^{3N}r d^{3N}p \tag{4}$$

and $w(E)$ is a weighting function which is prescribed by the ensemble we are interested in. Note that this is a weighting function, and not a probability. It is, thus, not normalized. In most Monte-Carlo simulations, only the integration over configuration space (the space spanned by the positions alone) is taken into account. The momenta are typically assumed to behave according to a Maxwell–Boltzmann distribution according to the temperature. In the most prominent example of the canonical ensemble

$$w(E) = \exp(-\beta E), \quad \beta = (k_B T)^{-1}. \tag{5}$$

However, equation (3) is valid independent of the ensemble. Most often transition probabilities are prescribed by the Metropolis algorithm [25] which satisfies detailed balance

$$\Pi(p,p') = \min\left\{1, \frac{w(E(p'))}{w(E(p))}\right\}. \tag{6}$$

The purpose of the DOS algorithm is to obtain a $\pi(E)$ which is independent of energy. We have to realize that in a simulation $\pi(E)$ is approximated by a histogram of energies. According to equation (3), we see that if we perform a simulation which realizes a flat histogram, the applied weight $w(E)$ is proportional to the inverse of the DOS. A flat histogram means that all energies are visited during the simulation with equal probability. Furthermore, we have to realize from basic statistical mechanics that by obtaining the DOS our problem is solved as all other properties can be derived from $\Omega(E)$. Moreover, if we eventually obtain a flat histogram, we cover the energy landscape homogeneously and do not get stuck in deep minima. During the process of obtaining the flat histogram, the simulation can get stuck and consequently sample only a local neighborhood of a minimum for some time but this happens less often than in standard simulations

Technically, the DOS algorithm starts with a guess of the DOS $\Omega_0(E)$ (which is often set to be uniform $\Omega_0(E) = c$) and performs a random walk in energy space using the Metropolis like acceptance criterion

$$\pi_{\text{acc}} = \min\left\{1, \frac{W^{\text{R}}_{\text{new}}\Omega'(E_{old})}{W^{\text{R}}_{\text{old}}\Omega'(E_{\text{new}})}\right\} \tag{7}$$

where W^{R} is the Rosenbluth weight of the corresponding move which has to be taken into account for biased techniques. After every move, the current estimate of the DOS for the energy the simulation is visiting $\Omega(E_{\text{visit}})$ is multiplied by a factor $f > 1$ to discourage further visits to this energy. This obviously violates detailed balance. However, f is decreased during the course of the simulation and the violation of detailed balanced is reduced. f is decreased and the energy histogram erased

when the histogram of energies is flat. Eventually, the convergence factor approaches $f = 1$ and detailed balance is restored [16].

The Wang–Landau algorithm yields the DOS $\Omega(E)$ without using a particular ensemble during the simulation. This provides the unique opportunity to analyze the results from the very same simulation in different ensembles. It has been identified earlier that by using histogram reweighting [26,27] simulations performed in a given ensemble can be analyzed using another or the same ensemble under different conditions. The DOS can be obtained and simulations can then be analyzed microcanonically even if the original simulation was performed in a canonical way [28]. The difference is that DOS simulations are *a priori* independent of any ensemble and target directly the DOS. There is no "best" or "natural" ensemble to analyze the data.

Statistical mechanics identifies the entropy as

$$S(E) = k_B \ln \Omega(E) \tag{8}$$

and this serves as direct connection to thermodynamics. One caveat is that the algorithm yields the DOS only to within a arbitrary constant. This is because the actual number of histogram entries is proportional to the length of the simulation. We only know the entropy exactly if we know the degeneracy of the ground state (or any other state). Otherwise, we obtain an entropy which is shifted by a constant

$$S'(E) = S(E) + S_0. \tag{9}$$

Using the microcanonical (*NVE*) ensemble we can use the original definition to obtain temperature

$$T^{-1}(E) = \partial_E S(E)|_{N,V}. \tag{10}$$

Note, that there is no temperature in the DOS simulation. The additive constant in the entropy is irrelevant here and for any other thermodynamic property. Inverting equation (10) yields the typically more interesting function $E(T)$ and by $c_V = T\partial_T S|_V$ or $c_V = \partial_T E(T)|_V$ we obtain the (isochoric) heat capacity in the microcanonical ensemble. This analysis is performed by numerically deriving the DOS or entropy with respect to energy after a completed DOS simulation. Any analysis may only be performed after the simulation is completed. Only then the DOS is known with the desired accuracy. This means that a running average over the simulation *does not* yield the correct value for any observable as the simulation does not reproduce representative members of the ensemble as a standard Monte-Carlo simulation but purely leads to the DOS in the end.

Most applications of the DOS algorithm use another way, the canonical method, to calculate properties. In the canonical (*NVT*) ensemble, the ensemble average of any property can be calculated from

$$\langle A(T)\rangle = \frac{\sum A(E)\Omega(E)\exp(-\beta E)}{\sum \Omega(E)\exp(-\beta E)}, \quad \beta = (k_B T)^{-1} \tag{11}$$

if the property A was recorded during the simulation as a function of energy. Energy and heat capacity can be calculated without additional measurements. They read

$$\langle E(T)\rangle = \frac{\sum \Omega(E) E \exp(-\beta E)}{\sum \Omega(E)\exp(-\beta E)} \tag{12}$$

$$\langle c_V(T)\rangle = \frac{\sum (E - \langle E(T)\rangle)^2 \Omega(E)\exp(-\beta E)}{\sum \Omega(E)\exp(-\beta E) k_B T^2}. \tag{13}$$

Other properties can be calculated from the canonical partition function or the free energy

$$\begin{aligned} F(N,V,T) &= -k_B T \ln Z_{\text{can}} \\ &= -k_B T \ln \int_{-\infty}^{\infty} \mathrm{d}E \Omega(E)\exp(-\beta E). \end{aligned} \tag{14}$$

Different ensembles are only required to be equivalent in the thermodynamic limit of infinitely large systems. This limit does not apply in a computer simulation with a finite system size. Therefore, a number of finite-size scaling algorithms have been introduced [29–31] to obtain properties in the thermodynamic limit.

2.2 Multiscale modeling of polymeric glass formers

Many industrially relevant glasses are polymeric. For example, a very abundant glass former is atactic polystyrene. However, it is well known that one of the most challenging problems in polymer simulations is the interplay of many different length scales. These range from atomic bonds to macroscopic length scales in applications. With different experimental techniques, this spectrum is readily covered. Structural and rheological characterization using neutron scattering [32,33], NMR spectroscopy [34], atomic force microscopy [35], thermodynamic studies [36] and many other methods obtained a detailed picture of the static and dynamic properties of polymeric systems from local mutual chain arrangements up to the behavior of the polymeric material in applications. The situation is different in theory and simulations, where techniques covering the whole range of length scales in a fully combined manner do not exist to date. Coarse-graining, the systematic mapping of various length scale models onto each other, has made significant progress in modeling homopolymers and polymers in solution [37–53]. Some very promising work in automating the mapping of microscale to mesoscale models [42,43,47,54,55] has demonstrated the potential of combining simulation techniques. There is a strong need for large scale models which keep a stronger identity of the underlying polymer in order to be able to quantitatively compare to experiments. Recently, it has been shown that such structurally coarse-grained systems can be used to estimate entanglement lengths of polymers, for polystyrene and polycarbonate [52,53].

The technique discussed here relies on the concept of superatoms. This means that a part of the polymer chain comprising a few atoms (typically 10–30) is represented

by one interaction center, a superatom. The interaction between superatoms carries implicitly the information of the interactions between the atoms. Although the choice of superatoms is arbitrary, in principal it is desirable that the distance between super-atoms along the chain is rigid defined as then effective harmonic bonds can be applied [48].

The iterative Boltzmann method (IBM) is a successful approach for structural coarse-graining of polymers [47,48,50,54]. It is designed to optimize a mesoscale model against the structure of an atomistic simulation. The method bases on radial distribution functions obtained from an atomistic simulation. In the limit of an infinitely diluted solution, one could use the potential of mean force gained by Boltzmann inverting the pair distribution function to get an interaction potential between monomers. However, in concentrated solutions, melts, or glasses the structure is defined by an interplay of the PMF with local packing effects. Thus, a direct application of the potential of mean force is not correct. Still the potential can be used by the IBM. A polymer melt is simulated in atomistic detail to obtain a pair distribution function. For low molecular weight systems, a direct simulation in the glassy system may be possible. We then start a mesoscale simulation only containing superatoms with an initial guess for the potential. Then the mesoscale simulation is analyzed and and the radial distribution functions are compared. Now a correction potential

$$\Delta V(r) = -k_{\mathrm{B}}T \ln \Delta \mathrm{RDF}(r) \tag{15}$$

is determined with the difference of distributions

$$\Delta \mathrm{RDF}(r) = \mathrm{RDF}_{\mathrm{atom}}(r) - \mathrm{RDF}_{\mathrm{meso}}(r). \tag{16}$$

It becomes immediately clear from this approach that the potential which results from this technique is completely numerical.

3. Applications of advanced methods to glass formers

After the presentation of the two techniques, we now show sample applications for glassy systems.

3.1 Simulations using DOSMC

We first show DOS simulations of a two-dimensional Ising system for various system sizes and analyze the results in terms of the canonical and the microcanonical ensemble to demonstrate the non-equivalence of ensembles from the same DOS. Additionally, we present the application of the algorithm to a model glass former.

3.1.1 Ising model. We performed simulations of the two-dimensional Ising model without magnetic field on a square lattice with $N \times N$ fields with $N \leq 64$. We realize that these are very small systems. Thus, they show the difference in finite size scaling more clearly and are therefore better for our purpose here. The energy in our units is

$$E = \sum_{\mathrm{pairs}} 0.5(A = B) \tag{17}$$

with A and B either 0 or 1 being the values of two neighboring fields which leads to $E_{\min} = 0$ and $E_{\max} = N^2$ for N. The critical temperature at which a phase transition occurs is in this set of units, i.e. coupling constant $J = 0.25$, $T_{\mathrm{c}} = 0.56725$ [56].

Our simulations use only simple spin flips which are trial moves that change the value of one field at a time. As acceptance is not a problem for this algorithm, more elaborate moves were not necessary. The simulations followed the original prescription of Wang and Landau [16], which begins with an initial DOS $\Omega(E) = 1$ for all macrostates. For numerical reasons, we store $(S/k_{\mathrm{B}}) = \ln \Omega(E)$.

We used the very strict criterion of the energy with the minimum number of visits being at least visited 99% of the average before we lower the convergence factor. This was done in order to maximize the accuracy at a given f in order to minimize overall runtime. The computer time per iteration increases dramatically with decreasing f if imperfections from earlier iterations are inherited. Of course, the energy states $E = 1$ and $E = N \times N - 1$ were disregarded since they cannot be achieved. We achieve the full calculation of the DOS of this system for $N = 16$ in 3 h on a Pentium 4 with 2 GHz.

The Ising model was simulated for all even system sizes between $N = 2$ and 32 as well as for a few larger systems and the corresponding densities of states were recorded. We calculated the heat capacities as described above in the canonical and the microcanonical way (cf. figure 1). In the case of the microcanonical heat capacity, we use running averages of five neighboring points after the derivative is taken, as the data is very noisy due to the numerical derivatives. Additionally, we performed a number of independent runs, where we initialized the random number generator differently and averaged over the resulting densities of states. The point of the maximum heat capacity was defined to be the transition temperature, as it is well defined in both ensembles. Using the canonical analysis, we could have determined the transition temperature by obtaining probability distributions for different temperatures. At a phase transition, the probability to be in the two phases is equal, thus, the area under the peaks corresponding to the different phases is equal. This equal-area condition has, however, no direct microcanonical counterpart.

For the same system size, the peaks in the heat capacity using the canonical definition is less sharp than in the microcanonical case. Especially, the peak heights are different. We do not reach peaks heights over $c_V = 2.5$ in the canonical case for system sizes of $N \leq 64$. However, the microcanonical ensemble readily reaches over $c_V = 3$ for $N = 20$. We clearly see the difference of ensembles.

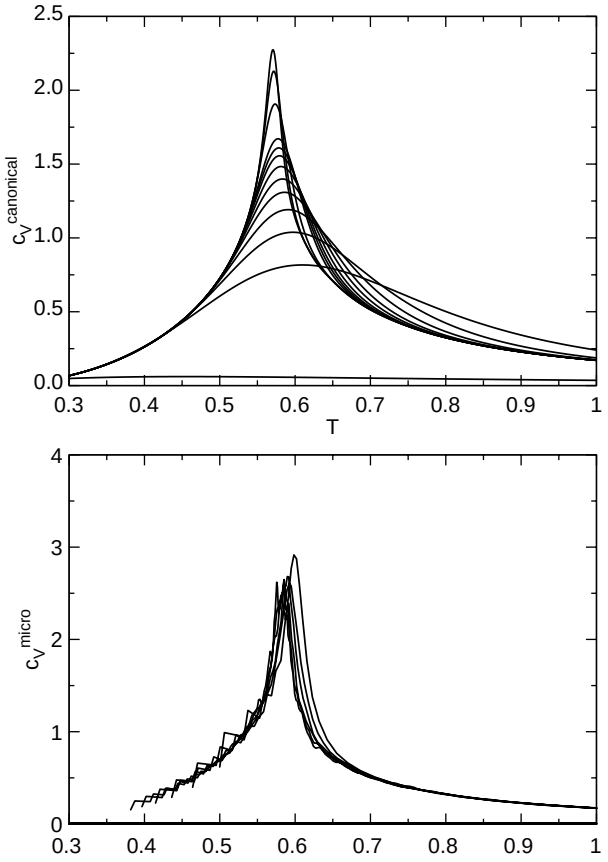

Figure 1. Canonical (top) and microcanonical heat capacity (both divided by N^2) for the two dimensional Ising model calculated using the same system. In the canonical case, we show $N = 2$, 4, 6, 8, 10, 12, 14, 16, 18, 20, 32, 48 and 64 from bottom to top. In the microcanonical case, we show $N = 10$, 12, 14, 16, 18 and 20.

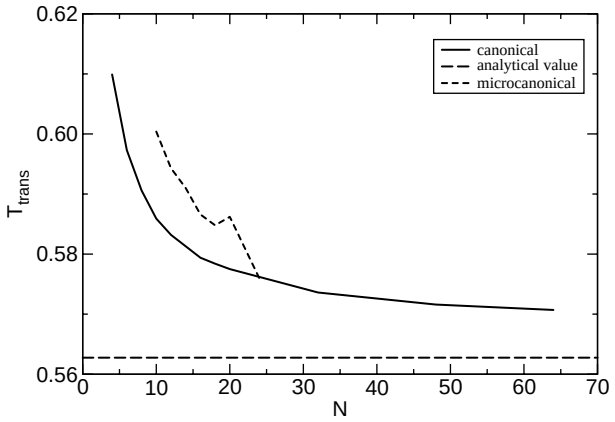

Figure 2. Canonical and microcanonical transition temperature (defined by the peak of the heat capacity) depending on system size for the two dimensional Ising model calculated using the same simulations.

We also observe that the transition temperature defined by the maximum of the heat capacity curve is generally higher using the microcanonical analysis than in the canonical case (figure 2). This suggests that the canonical transition temperature is a better estimate of the infinite size transition temperature even as the heat capacity is not as sharply defined. We have to point out, however, that the microcanonical analysis suffers from numerical difficulties due to the nature of numerical derivatives. This could lead to the effect of missing small features. If the statistical accuracy of the DOS is not extremely well converged, then the canonical ensemble analysis is by its intrinsic additional averaging generally superior.

3.1.2 Model glass. The effects of different ensembles are not limited to simple lattice systems but apply to glasses as well. This is especially noteworthy, as in the simulation literature often glassy systems with very few particles are studied [6] such that large practical implications can be expected. We determined the energy vs temperature curve for a simple model glass former [57]. We recently studied the system using DOS Monte-Carlo [12]. The data presented here is independent of the earlier study. The model consists of a binary mixture of Lennard–Jones particles, 80% A and 20% B. A total of 250 particles is used in our calculations as even with such a powerful technique the simulation lengths are prohibitive. The interaction parameters between particles of species A and B are $\epsilon_{AA} = 1.0$ and $\sigma_{AA} = 1.0$, $\epsilon_{BB} = 0.5$ and $\sigma_{BB} = 0.88$ and $\epsilon_{AB} = 1.5$ and $\sigma_{AB} = 0.8$. The density is $1.204\sigma_{AA}^{-3}$. We use particle identity swap and simple translation moves for this system. For this model, it was actually extremely difficult to get flat histograms over the very wide energy region from -1850 to -1400 which covers the relevant temperature ranges. First, we performed simulations in 18 small overlapping energy windows ($-1850 \rightarrow -1800$, $-1825 \rightarrow -1775$ and so on). After obtaining the DOS in the individual windows, we joined them by shifting the DOS to overlap in the common energy ranges, which resulted in a singled DOS. We did not try to push for $f < 10^{-5}$ but after we obtained the DOS for the whole range we continued to update it at $f = 10^{-5}$ for more than 2 million steps. Once the DOS covered almost the full energy range we found the final DOS from which the subsequent analysis started. We show in figure 3, the comparison of the energy using the microcanonical and canonical analysis for the binary Lennard–Jones glass. The energy curves are very similar. In figure 3, we also show the comparison of the canonical and microcanonical heat capacities using the approaches mentioned earlier. Although the numerical derivative of the microcanonical data is very noisy, we still see a clear trend comparable to the canonical data. At very low temperatures (energies) even the DOS technique has difficulties to converge perfectly leading to weak noise in the canonical heat capacity as well.

We find a peak in the heat capacity and a kink in the energy vs temperature. This is consistent with findings of Grigera *et al.* for a related glass former [6]. In that case, the transition temperature was very close to the theoretical Kauzmann temperature. As we do not find any hints for a structural transition, we can conclude that we find a transition reminiscent of a glass transition although the nature of the transition is not completely clear yet. Our transition temperature is actually very close and

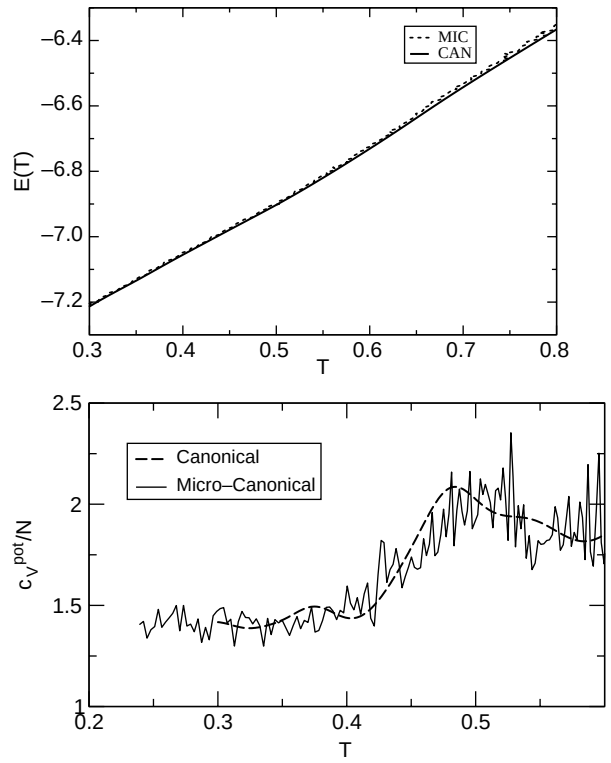

Figure 3. Top: canonical and microcanonical potential energy as a function of temperature of a binary Lennard–Jones glass. Lower: heat capacities.

in agreement with earlier data of mode coupling temperature data [58]. The study in both ensembles shows qualitatively similar results but the quantitative data are slightly different.

3.2 Results of the coarse grained glasses

We now show how multiscale modeling can help in the understanding of a polymer under cooling. We developed a model for the glass former polystyrene (PS) [50] using the iterative Boltzmann technique. In figure 4, we show the resulting potential.

The atomistic simulations on which the model is based have been performed at 450 K using the forcefield from [59]. The atomistic systems contained 24 chains of length 15 monomers. Coarse-grained simulations have been performed for various chain lengths between 15 and 240 monomers [53]. All the coarse-grained data presented here is simulated at chain length $N = 30$. The temperature and pressure of the atomistic simulations are kept constant using Berendsen's weak coupling method [60]. The coarse-grained simulations are performed under constant volume and the temperature is kept constant by using Brownian dynamics. As the coarse-graining approach obtains a potential under the same conditions as the atomistic simulations ($T = 450$ K, $p = 101.3$ kpa) it is not clear how such a model fares under different conditions, e.g. at different temperatures. We also performed some simulations at 380 K [61]. The atomistic simulations have been performed for atactic and randomly polymerized polystyrene. As the RDFs in the melt and the glass are expected to be similar, we trust that simulations of our model can estimate the behavior at lower temperatures. Polystyrene is a good glass former; the application of the mesoscale model to polystyrene glasses is an independent critical test of this approach.

Figure 5 shows the radial distribution functions of PS chains at various temperatures. Here, as in all other

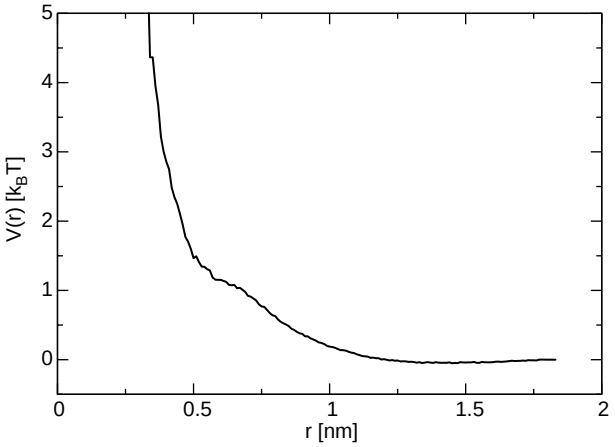

Figure 4. Interaction potential for polystyrene monomers.

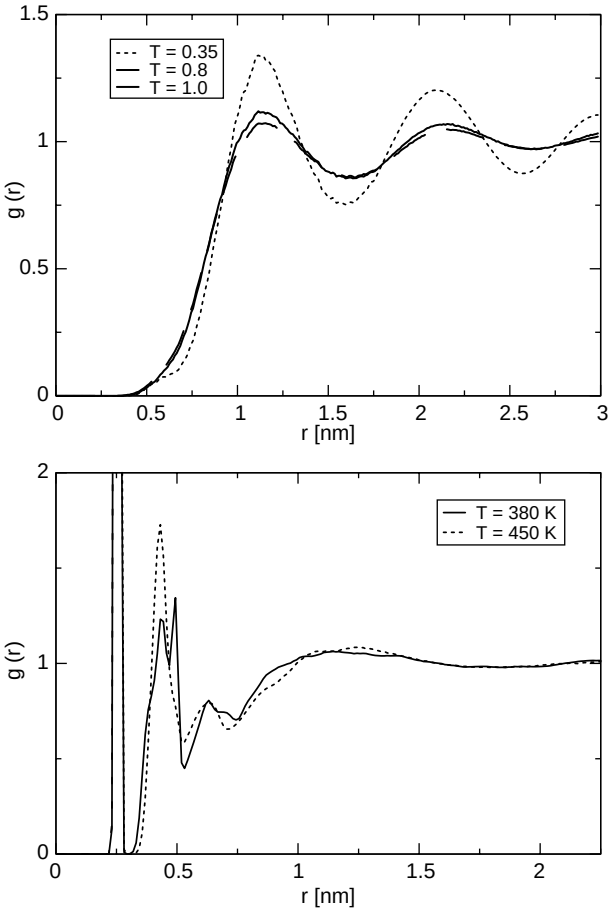

Figure 5. Radial distribution functions between monomers of polystyrene at different temperatures. Top: mesoscale model (30 monomers). Lower: atomistic simulations (15 monomers). Note that for the atomistic simulations the intramolecular contributions have not been taken out for statistical reasons.

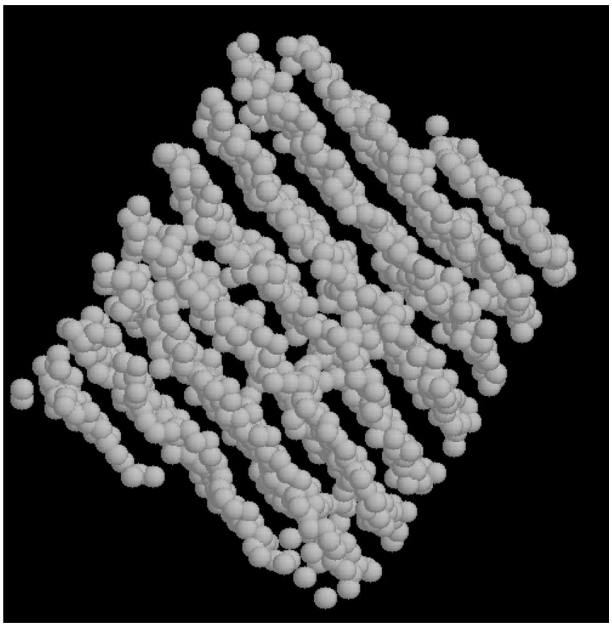

Figure 6. Snapshot of the coarse-grained simulation at $T = 0.35$. The system clearly shows signs of crystallinity.

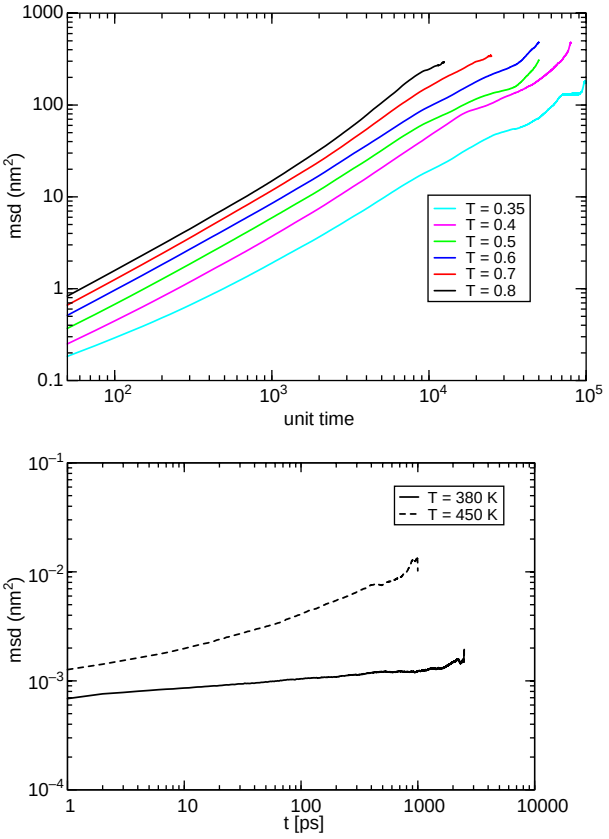

Figure 7. Left: mean squared displacement of mesoscale polystyrene (30 monomers) at different temperatures. Right: atomistic mean-squared displacements of polystyrene with chain length 15 monomers.

figures, the atomistic simulations are performed for chains of length 15 and the mesoscale chains have length 30. The dimensionless temperature $T = 1$ corresponds to the melt at which the system was optimized. The radial distribution functions actually depend slightly on chain length for the mesoscale model. At $T \geq 0.8$, we observe a clear melt structure and with lowering temperature the structure gets more pronounced. At the lowest temperature it shows clear signs of crystallinity (cf. figure 6). The temperature effect on the mesoscale model is stronger than expected for a glass forming system and it apparently has a tendency to crystallize. This clearly shows that the analysis of a mesoscale model under changed conditions has to be taken with caution.

We now analyse the dynamics of the atomistic and the mesoscale model at selected temperatures. Figure 7 shows the mean-squared displacements for atomistic and mesoscale PS. The corresponding diffusion coefficients for the mesoscale model are found in table 1. Clearly, lowering the temperature has a slowing effect on the dynamics in both models. In the mesoscale case, there is some evidence for a qualitative change at low temperatures. For $T = 0.35$, the mean squared displacement is no more parallel to the higher temperatures. There is a transition (possibly crystallization) taking place. However, this transition is clearly lower than the experimental glass transition temperature. If we map the atomistic temperature of 450 K to $T = 1$ in the mesoscale model we obtain a dynamic change around 150 K which is far below the glass transition temperature of 373 K for atactic PS. The atomistic simulations at 380 K show a clear slowing down as well and are in qualitative agreement with the expected glass temperature. This indicates that the dynamical mapping needs be improved. In order to remove the tendency of crystallization probably a distinction between meso and racemo dyads needs to be added as well.

Analyzing the mean-squared displacements of the center of geometry of chains from atomistic simulations we have to take into account that the data at 380 K is a random mixture of head-to-head and head-to-tail polystyrene, whereas, at 450 K the polystyrene is an atactic configuration. However, the difference between these is only expected to be minor. Much more important is the strong temperature influence. The lower temperature is just above the glass transition temperature. Clearly, atomistic simulations of 5–10 ns are too short for coming even close to equilibration. A coarse-grained approach is clearly needed. However, the atomistic simulations at the lower temperature exhibit a plateau-like dynamics indicating a cage effect. The length scales in figure 7 have been mapped by the distance of peaks in the

Table 1. Diffusion constants (D) of PS chain length of 30 at various temperatures.

Temperature	*D* (10^{-5} *cm*^{2}*/s*)
0.35	0.3697
0.4	0.9968
0.5	1.5950
0.6	2.5229
0.7	2.7673
0.8	3.1590
1.0	3.6787

potentials and radial distribution functions. We refrained from mapping the time-scales as it would be ambiguous. For this longer atomistic simulations reaching into free diffusion would be highly desirable

In summary, the mesoscale model developed for polystyrene melts can help in a description of the glass transition of polystyrene but an improved model will be necessary for a more quantitative description.

4. Conclusions and outlook toward a combination of the approaches

It is clear that both DOS Monte-Carlo as well as multiscale modeling are important techniques which can help in the understanding of the glass transition. It also becomes clear that the modeling of the glass transition even with such advanced techniques is still not in a satisfactory state and much remains to be done.

We showed that DOS Monte-Carlo has in addition to its well-known benefits, the advantage that one can investigate the same system in different ensembles. It allows us to demonstrate different finite size scalings in small Ising systems. We showed that also for a simple off-lattice system these effects are noticeable if the system size is small enough. Especially, in the area of simulations of model glasses small system sizes where even less than 100 particles are regularly discussed [6,13] the effect of different ensembles becomes important.

We also see that for systems where the structure and dynamics changes only slightly between different conditions, we can use the potential over a larger temperature range.

Let us conclude with an outlook to the combination of the two techniques. We performed atomistic simulations of ortho-terphenyl (OTP) at various temperatures. The details will be published elsewhere [62]. Figure 8 shows the mean squared displacements of these molecules at high and low temperatures. Clearly, below $T_g \approx 260\,K$ [62] a glass plateau is observed. But even for a small glass former simulations for more than 10 ns become very tedious. So we determined the radial distribution functions

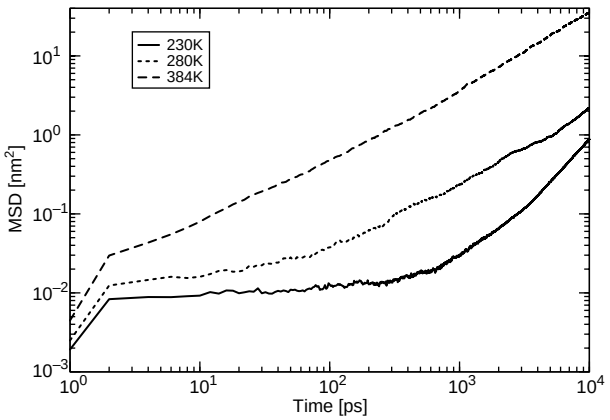

Figure 8. Mean squared displacement of atomistic OTP at different temperatures.

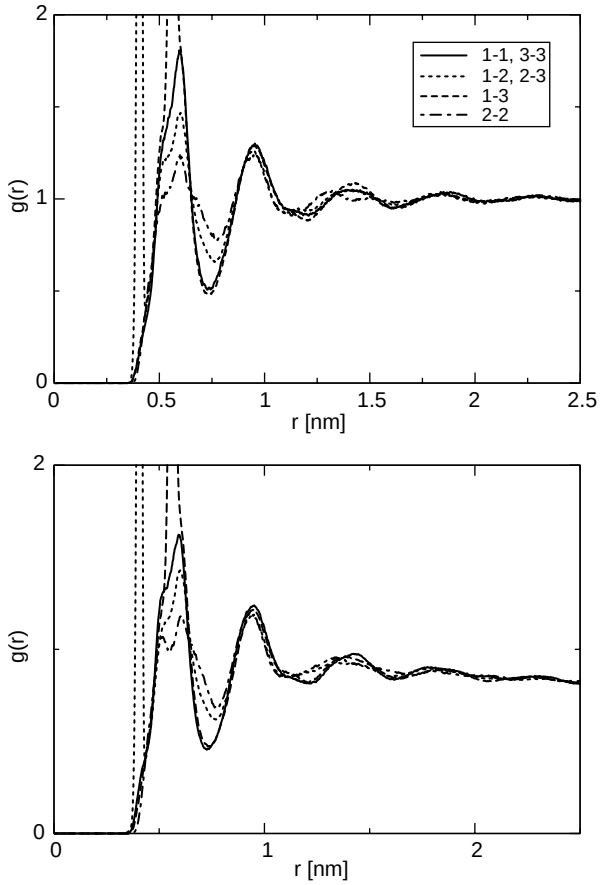

Figure 9. Radial distribution functions of OTP glasses at 230 K between the different rings. one and three are the outer rings, two is the central ring. Running averages have been applied. Left: bulk, Right: thin Film. The legend in the left figure applied to both graphs.

of the rings of OTP as prerequisite for coarse-graining. Figure 9 shows these radial distribution function in bulk and in a free standing film at 230 K, which is below the glass transition ($\approx 260\,K$ for this model). We see that the RDFs are very similar, thus, giving promise that the coarse-graining from the bulk is also applicable for thin films. Moreover, we found that the radial distribution function and structure factor of OTP is almost independent of temperature over a very wide temperature range [62]. This suggests that the structural mesoscale model should be better applicable for the glass study than in the case of polystyrene as the problem of tacticity does not interfere in that case. As a coarse-grained OTP will have only three sites a DOS Monte-Carlo calculation both in bulk and free standing films will be possible. This will pave the way for future studies of even more complicated glass formers.

Acknowledgements

This work was partially supported by the US Department of Energy, Office of Science, Office of Advanced Scientific Computing Research (grant DE-FG02-03ER25568). This research also used resources of the National Energy Research Scientific Computing Center, which is supported by the Office of Science of the U.S.

Department of Energy under Contract No. DE-AC03-76SF00098.

References

[1] M.D. Ediger, C.A. Angell, S.R. Nagel. Supercooled liquids and glasses. *J. Phys. Chem.*, **100**, 13200 (1996).

[2] P.G. Debenedetti, F.H. Stillinger. Supercooled liquids and the glass transition. *Nature*, **410**, 259 (2001).

[3] M. Mezard, G. Parisi. Thermodynamics of glasses: a first principles computation. *Phys. Rev. Lett.*, **82**, 747 (1999).

[4] J.H. Gibbs, E.A. DiMarzio. Nature of the glass transition and the glassy state. *J. Chem. Phys.*, **28**, 373 (1958).

[5] B. Coluzzi, G. Parisi, P. Verrocchio. Thermodynamical liquid-glass transition in a Lennard–Jones binary mixture. *Phys. Rev. Lett.*, **84**, 306 (2000).

[6] T.S. Grigera, G. Parisi. Fast Monte-Carlo algorithm for supercooled soft spheres. *Phys. Rev. E*, **63**, 045102(R) (2001).

[7] L. Santen, W. Krauth. Absence of thermodynamic phase transition in a model glass former. *Nature*, **405**, 550 (2000).

[8] W. Götze, L. Sjögren. Relaxation processes in supercooled liquids. *Rep. Prog. Phys.*, **55**, 241 (1992).

[9] S. Kamath, R.H. Colby, S.K. Kumar, J. Baschnagel. Thermodynamic signature of the onset of caged dynamics in glass-forming liquids. *J. Chem. Phys.*, **116**, 865 (2002).

[10] S. Mossa, E. La Nave, H.E. Stanley, C. Donati, F. Sciortino, P. Tartaglia. Dynamics and configurational entropy in the Lewis–Wahnstrom model for supercooled orthoterphenyl. *Phys. Rev. E*, **65**, 041205 (2002).

[11] K. Binder, J. Baschnagel, W. Paul. Glass transition of polymer melts: test of theoretical concepts by computer simulation. *Prog. Polym. Sci.*, **28**, 115 (2003).

[12] R. Faller, J.J. dePablo. Density of states of a binary Lennard–Jones glass. *J. Chem. Phys.*, **119**, 4405 (2003).

[13] S. Büchner, A. Heuer. Potential energy landscape of a model glass former: thermodynamics, anharmonicities, and finite size effects. *Phys. Rev. E*, **60**, 6507 (1999).

[14] B. Coluzzi, G. Parisi, P. Verocchio. Lennard–Jones binary mixture: a thermodynamical approach to glass transition. *J. Chem. Phys.*, **112**, 2933 (2000).

[15] F. Sciortino, W. Kob, P. Tartaglia. Thermodynamics of supercooled liquids in the inherent-structure formalism: a case study. *J. Phys: Condens. Matter*, **12**, 6525 (2000).

[16] F. Wang, D.P. Landau. Efficient, multiple-range random walk algorithm to calculate the density of states. *Phys. Rev. Lett.*, **86**, 2050 (2001).

[17] F. Wang, D.P. Landau. Determining the density of states for classical statistical models: a random walk algorithm to produce a flat histogram. *Phys. Rev. E*, **64**, 056101 (2001).

[18] T.S. Jain, J.J. de Pablo. Calculation of density of states for free-standing polymer films using configurational bias. *J. Chem. Phys.*, **116**, 7238 (2002).

[19] N. Rathore, J.J. de Pablo. Monte-Carlo simulation of proteins through a random walk in energy space. *J. Chem. Phys.*, **116**, 7225 (2002).

[20] Q. Yan, R. Faller, J.J. de Pablo. Density of states Monte-Carlo method for simulation of fluids. *J. Chem. Phys.*, **116**, 8745 (2002).

[21] Q. Yan, J.J. de Pablo. Fast calculation of the density of states of a fluid by Monte-Carlo simulations. *Phys. Rev. Lett.*, **90**, 035701 (2003).

[22] M. Troyer, S. Wessel, F. Alet. Flat histogram methods for quantum systems: algorithms to overcome tunnelling problems and calculate the free energy. *Phys. Rev. Lett.*, **11**, 120201 (2003).

[23] M.S. Shell, P.G. Debenedetti, A.Z. Panagiotopoulos. An improved Monte-Carlo method for direct calculation of the density of states. *J. Chem. Phys.*, **119**, 9406 (2003).

[24] P.M.C. de Oliveira, T.J.P Penna, H.J. Herrmann. Broad histogram method. *Braz. J. Phys.*, **26**, 677 (1996).

[25] N. Metropolis, A.W. Rosenbluth, M.N. Rosenbluth, A.H. Teller, E. Teller. Equation of state calculations by fast computing machines. *J. Chem. Phys.*, **21**, 1087 (1953).

[26] A.M. Ferrenberg, R.H. Swendsen. New Monte-Carlo technique for studying phase transitions. *Phys. Rev. Lett.*, **61**, 2635 (1988).

[27] A.M. Ferrenberg, R.H. Swendsen. Optimized Monte-Carlo data analysis. *Phys. Rev. Lett.*, **63**, 1195 (1989).

[28] M. Pleimling, A. Hüller. Crossing the coexistence line at constant magnetization. *J. Stat. Phys.*, **104**, 971 (2001).

[29] K. Binder. *Phase Transitions and Critical Phenomena*, vol. 5B, chap. Monte-Carlo investigations of phase transitions and critical phenomena, Academic Press, New York (1976).

[30] J.G. Brankov. *Introduction to Finite Size Scaling*, vol. 08 of Leuven Notes in Mathematical and Theoretical Physics, Leuven University Press, Leuven (1996).

[31] M. Pleimling, A. Behringer, A. Hüller. Microcanonical scaling in small systems. *Phys. Lett. A*, **328**, 432 (2004).

[32] B. Frick, D. Richter. The microscopic basis of the glass transition in polymers from neutron scattering studies. *Science*, **267**, 1939 (1995).

[33] B. Ewen, D. Richter. Neutron spin echo investigations on the segmental dynamics of polymers in melts, networks and solutions. *Adv. Polym. Sci.*, **134**, 1 (1997).

[34] K. Schmidt-Rohr, H.W. Spiess. *Multidimensional Solid State NMR and Polymers*, Academic Press, New York (1994).

[35] D. Parrat, F.S.J.M. Solleti, T.M. Due. Imaging modes in atomic-force microscopy. *J. Trace Microprobe Tech.*, **13**, 343 (1995).

[36] Y. Einaga. Thermodynamics of polymer solutions and mixtures. *Prog. Polym. Sci.*, **19**, 1 (1994).

[37] J.D. McCoy, J.G. Curro. Mapping of explicit atom onto united atom potentials. *Macromolecules*, **31**, 9362 (1998).

[38] M. Murat, K. Kremer. From many monomers to many polymers: soft ellipsoid model for polymer melts and mixtures. *J. Chem. Phys.*, **108**, 4340 (1998).

[39] W. Tschöp, K. Kremer, J. Batoulis, T. Bürger, O. Hahn. Simulation of polymer melts. I. Coarse-graining procedure for polycarbonates. *Acta Polym.*, **49**, 61 (1998).

[40] J. Eilhard, A. Zirkel, W. Tschöp, O. Hahn, K. Kremer, O. Schärpf, D. Richter, U. Buchenau. Spatial correlations in polycarbonates: neutron scattering and simulation. *J. Chem. Phys.*, **110**, 1819 (1999).

[41] J. Baschnagel, K. Binder, P. Doruker, A.A. Gusev, O. Hahn, K. Kremer, W.L. Mattice, F. Müller-Plathe, M. Murat, W. Paul, S. Santos, U.W. Suter, V. Tries. Bridging the gap between atomistic and coarse-grained models of polymers: status and perspectives. *Adv. Polym. Sci.*, **152**, 41 (2000).

[42] H. Meyer, O. Biermann, R. Faller, D. Reith, F. Müller-Plathe. Coarse graining of nonbonded interparticle potentials using automatic simplex optimization to fit structural properties. *J. Chem. Phys.*, **113**, 6264 (2000).

[43] R.L.C. Akkermans, W.J. Briels. A structure-based coarse-grained model for polymer melts. *J. Chem. Phys.*, **114**, 1020 (2001).

[44] K.R. Haire, T.J. Carver, A.H. Windle. A Monte Carlo lattice model for chain diffusion in dense polymer systems and its interlocking with molecular dynamics simulations. *Comp. Theor. Polym. Sci.*, **11**, 17 (2001).

[45] C.F. Abrams, K. Kremer. Effects of excluded volume and bond length on the dynamics of dense bead-spring polymer melts. *J. Chem. Phys.*, **116**, 3162 (2002).

[46] R. Faller, F. Müller-Plathe. Multi-scale modelling of poly(isoprene) melts. *Polymer*, **43**, 621 (2002).

[47] R. Faller, D. Reith. Properties of polyisoprene—Model building in the melt and in solution. *Macromolecules*, **36**, 5406 (2003).

[48] R. Faller. Automatic coarse graining of polymers. *Polymer*, **45**, 3869 (2004).

[49] M. Tsige, J.G. Curro, G.S. Grest, J.D. McCoy. Molecular dynamics simulations and integral equation theory of alkane chains: comparison of explicit and united atom models. *Macromolecules*, **36**, 2158 (2003).

[50] Q. Sun, R. Faller. Systematic coarse-graining of atomistic models for simulation of polymeric systems. *Comput. Chem. Eng.*, **29**, 2380 (2005).

[51] R. Faller. Coarse-grain modeling of polymers. *Rev. Comput. Chem.*, in press for Volume **23** (2006).

[52] S. Leon, N. van der Vegt, L. Delle Site, K. Kremer. Bisphenol a polycarbonate: entanglement analysis from coarse-grained MD simulations. *Macromolecules*, **38**, 8078 (2005).

[53] Q. Sun, R. Faller. Crossover from unentangled to entangled dynamics in a systematically coarse-grained polystyrene melt. *Macromolecules*, **39**, 812 (2006).

[54] D. Reith, H. Meyer, F. Müller-Plathe. CG-OPT: a software package for automatic force field design. *Comput. Phys. Commun.*, **148**, 299 (2002).

[55] H. Fukunaga, J. Takimoto, M. Doi. A coarse-graining procedure for flexible polymer chains with bonded and nonbonded interactions. *J. Chem. Phys.*, **116**, 8183 (2002).

[56] L. Onsager. Crystal statistics. I. A two-dimensional model with an order-disorder transition. *Phys. Rev.*, **65**, 117 (1944).

[57] W. Kob, H.C. Andersen. Scaling behavior in the β-relaxation regime of a supercooled Lennard–Jones mixture. *Phys. Rev. Lett.*, **73**, 1376 (1994).

[58] R. Yamamoto, W. Rob. Replica exchange molecular dynamics simulation for supercooled liquids. *Phys. Rev. E*, **61**, 5473 (2000).

[59] Q. Sun, R. Faller. Molecular dynamics of a polymer in mixed solvent: atactic polystyrene in a mixture of cyclohexane and N,N-dimethylformamide. *J. Phys. Chem. B*, **109**, 15714 (2005).

[60] H.J.C. Berendsen, J.P.M. Postma, W.F. van Gunsteren, A. DiNola, J.R. Haak. Molecular dynamics with coupling to an external heat bath. *J. Chem. Phys.*, **81**, 3684 (1984).

[61] F.R. Pon, Q. Sun, R. Faller. Detailed molecular modelling study on the local dynamics in polyisoprene-polystyrene blends, in preparation (2005).

[62] J. Ghosh, R. Faller. A comparative molecular simulation study of the glass former ortho-terphenyl in bulk and free standing films, submitted to *J. Chem. Phys.* (2005).